

# MOPITT Geolocation Bias Analysis and Corrections

Merritt N. Deeter\*

MOPITT Algorithm Development Team

Atmospheric Chemistry Division

National Center for Atmospheric Research

Boulder, CO 80307

Last Revised June 7, 2012

\* contact at [mnd@ucar.edu](mailto:mnd@ucar.edu)

# Table of Contents

1 Overview.....	3
1.1 Level 1 Processing.....	3
1.2 Observed Geolocation Bias.....	3
1.3 Physical Interpretation.....	7
2 Correction Method.....	8
2.1 Method for Quantifying Geolocation Bias.....	8
2.2 Method for Quantifying Viewing Angle Bias.....	10
2.3 Level 1 Processor Revisions.....	10
3 Additional Effects.....	10
3.1 Related Geometrical Data.....	10
3.2 Cloud Detection.....	11
3.3 Retrieval Processing.....	11
3.4 Level 3 Products.....	11
4 Verification.....	11
4.1 Latitude and Longitude Error Statistics.....	12
4.2 Daytime Overpasses.....	13
4.3 Nighttime Overpasses.....	13
4.4 Cloud Diagnostics.....	14
5 Summary.....	14
6 Appendix.....	16

# 1 Overview

MOPITT Level 1 (calibrated radiances) and Level 2 (retrieval products) data products include geolocation data (latitude and longitude values) for each MOPITT observation. The MOPITT team has recently determined that geolocation data in all MOPITT Level 1 and Level 2 products (including Versions 3, 4, and 5) include a potentially significant bias. In daytime overpasses, the magnitude of the geolocation bias is approximately 0.35 degrees longitude, somewhat larger than the size of a single MOPITT pixel. Satellite zenith angle and solar zenith angles values, which are also included in the MOPITT Level 1 and Level 2 data files, are also slightly biased as the result of the geolocation bias. Gridded Level 3 data should also be affected by this bias since the grid-cell assignment of individual Level 2 observations is based on the geolocation data.

This document presents an analysis of the geolocation bias along with a method developed for eliminating the bias in future MOPITT products, beginning with the Version 6 product. For consistency, the current Version 5 product will continue to be processed with the known geolocation bias.

## 1.1 Level 1 Processing

Within the MOPITT Level 1 Processor, latitude and longitude values for each observation are determined by calls to the "Toolkit." Parameters needed by the Toolkit include the exact time of the observation and viewing angle offsets which, for the MOPITT instrument, are dependent only on the stare index (between one and 29) and the pixel index (between one and four). The Toolkit software also accesses attitude and ephemeris data which describe the exact position and orientation of the Terra platform at all times.

MOPITT viewing angle offsets for each pixel/stare combination are fixed within the Level 1 Processor and are expressed as direction cosines referenced to the instrumental x-y-z coordinate system. These offset angles appear in the file 'MOPIP.txt.' The nominal values for these offsets, which have been used for all operational processing from 2000-2012 (i.e., for the MOPITT Version 3, 4, and 5 products) are based on the assumption that the MOPITT instrument itself is exactly aligned with the x-y-z coordinate system for Terra. The results presented below in Sec. 2 indicate a misalignment of the MOPITT instrument of several degrees.

## 1.2 Observed Geolocation Bias

The geolocation bias was first reported by Matthieu Pommier from Environment Canada in February, 2012. By gridding and averaging multiple years of MOPITT retrieval data, he found that MOPITT CO distributions for several megacities appear systematically shifted to the west of their expected locations. Similar analyses of IASI CO retrievals did not show this bias. His analysis indicated a geolocation bias of approximately 0.3 degrees longitude.

Even without averaging multiple MOPITT overpasses, geolocation errors are evident in maps of both calibrated radiances and retrieval products. The errors are particularly obvious in daytime near-infrared (NIR) radiance maps of regions where coastlines provide sharp contrast between bright land and dark ocean. For those same scenes, geolocation errors are also often clearly evident in retrieved surface temperature. Geolocation errors are more readily observed in daytime (descending) overpasses than in nighttime (ascending) overpasses because (1) NIR radiances are dependent on reflected solar radiation

and are therefore not informative for nighttime overpasses and (2) TIR radiances in nighttime overpasses are often similar over water and land because of similar surface temperatures.

Figure 1 below shows MOPITT Channel 6A radiances for a daytime overpass of an area including the eastern Mediterranean Sea (in the northwest quadrant) and northern Red Sea (in the center-south). Channel 6 is the MOPITT NIR channel for CO. The top panel shows the current Version 5 product. The bottom panel shows the same observations processed with the geolocation correction method described in Section 2. Coastlines plotted in these maps are generated by IDL. Inspection of the top panel in Fig. 1 indicates that the radiances along the coastlines of both the Mediterranean and Red Sea are shifted to the west of their expected positions. For example, very low NIR radiances indicating water are clearly observed to the west of the western coastline of the Red Sea between about 24N and 30N. The opposite effect occurs on the eastern coastline of the Red Sea where relatively large radiances indicating land are actually observed over water. There is no obvious indication of a geolocation bias in the north-south direction.

Figure 2 shows maps of retrieved surface temperature for the same scene. MOPITT retrievals of surface temperature depend primarily on Channel 5A and 5D thermal-infrared (TIR) radiances. As in Fig. 1, the top panel of Fig. 2 presents surface temperature retrievals for the Version 5 product, while the lower panel presents results based on corrected geolocation data. In the top panel, low surface temperatures representative of water are observed to the west of the western coastline of the Red Sea while very high surface temperatures representing land are observed over water. Comparison of the top panels of Figures 1 and 2 suggests that Channels 5 and 6 are both affected by a geolocation bias of approximately the same magnitude and direction.



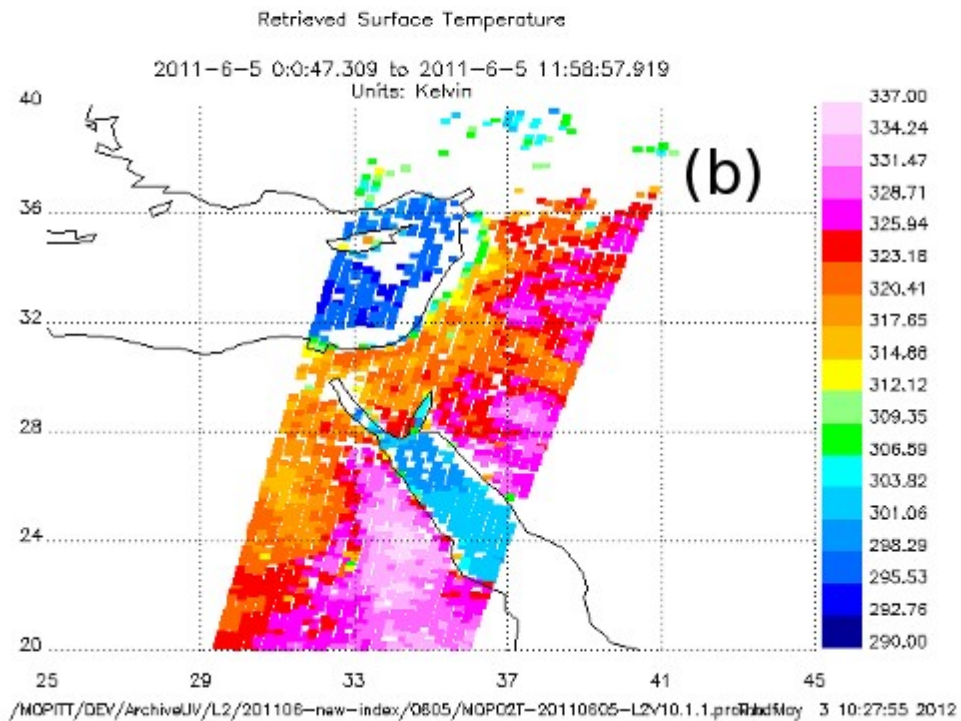
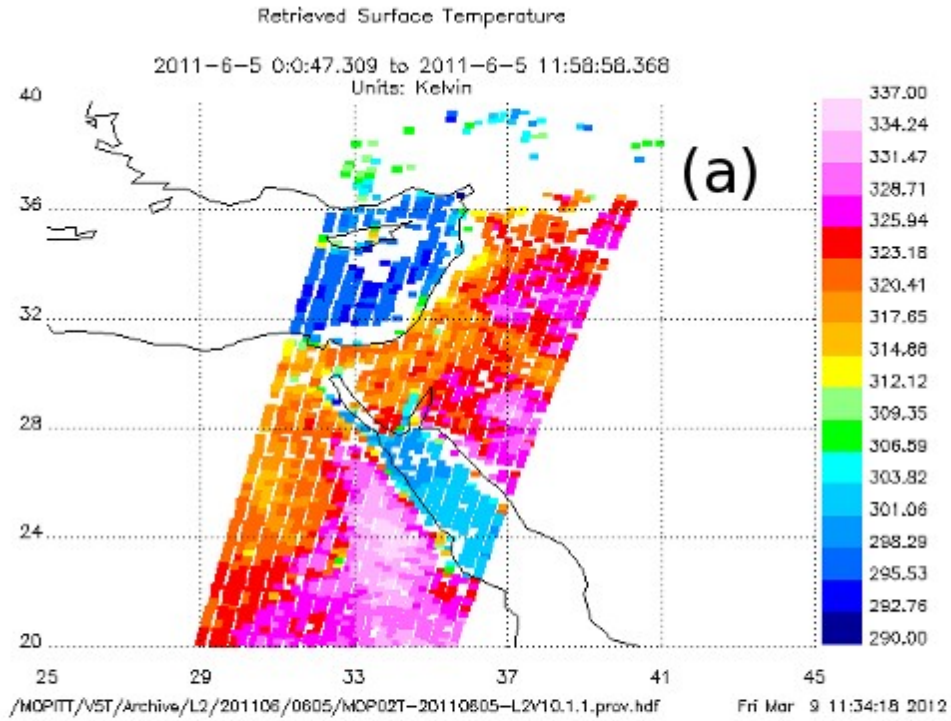


Figure 2. Retrieved surface temperatures for same scene described in Fig. 1. Surface temperatures along coastlines in V5 product shown in top panel (a) appear systematically shifted to the west by at least one MOPITT pixel. Geocorrected product shown in bottom panel (b) exhibits clear improvement.

### 1.3 Physical Interpretation

A diagram depicting the MOPITT geolocation bias is shown in Figure 3. The black lines indicate the sub-satellite tracks of Terra. In daytime (descending) overpasses, Terra travels from the northeast to the southwest. In nighttime (ascending) overpasses, Terra travels from the southeast to the northwest. (Terra is a sun-synchronous polar-orbiting satellite with an orbital inclination of 98.2 degrees.) The blue squares represent the actual location of a particular MOPITT field of view (FOV) whereas the yellow squares represent the reported (biased) location. The solid red vector represents the error vector from the true location of the FOV to the reported location. This vector can be resolved into two components referenced to Terra's coordinate system: an 'along-track' component and a 'cross-track' component. These component vectors are shown as dashed red vectors.

The most likely source of the geolocation bias is a simple viewing angle bias resulting from a misalignment between the MOPITT instrument and the Terra platform. Observations indicate that the geolocation bias in daytime overpasses is almost purely longitudinal. As indicated by the left side of the Figure, this suggests that the viewing angle bias in the Terra reference frame includes a small along-track angular bias and a larger cross-track angular bias. For nighttime overpasses, this model predicts that the combined effects of the along-track and cross-track angular biases will result in an error vector pointing to the northeast. Thus, in contrast with daytime overpasses, nighttime geolocation errors should exhibit significant latitudinal and longitudinal components.

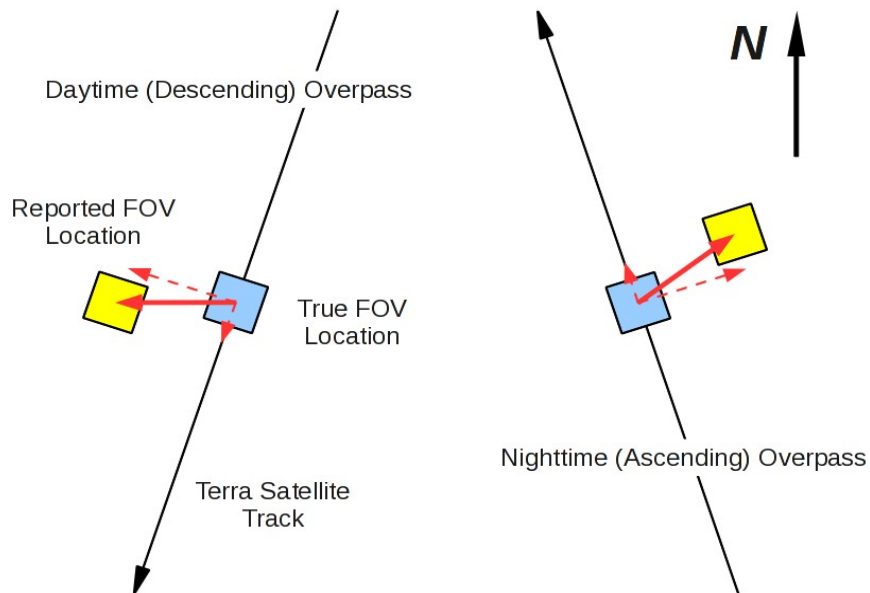


Figure 3. Diagram depicting MOPITT geolocation bias in daytime (left) and nighttime (right) overpasses.

## 2 Correction Method

### 2.1 Method for Quantifying Geolocation Bias

Analyses of MOPITT observations in individual overpasses (as presented in Figs. 1 and 2) are only sufficient for coarsely estimating the actual geolocation bias. To resolve the bias with high accuracy, information from many overpasses must be exploited. Also, instead of relying on coastlines plotted by IDL, the geographical boundaries between ocean and land can be more precisely determined using the DEM-based 'Surface Index' diagnostic included in the MOPITT Level 2 Product. Thus, a methodology for estimating the geolocation bias (including both latitudinal and longitudinal components) has been developed based on finely-gridded clear-sky NIR radiance values and corresponding surface index values. The underlying assumption is that for a scene including both land and water, the mean NIR radiance over water should be minimized with respect to latitudinal and longitudinal shifts.

As the initial step, finely-gridded NIR (6A) radiance maps of selected regions were generated by gridding and averaging all clear-sky observations over that region in a given year. Exclusion of cloudy observations was achieved by extracting the radiances from the 'Level 1 Radiances and Errors' diagnostic in the MOPITT V5 Level 2 files rather than the actual Level 1 radiance files. A grid resolution of 0.05 degrees was used for both latitude and longitude. This resolution represents a tradeoff between geolocation bias precision, which favors finer grids and statistically robust gridded radiances, which favors coarser grids. Surface index maps were also generated by gridding and averaging all of the surface index values corresponding to the 6A radiance values. A surface index value of 1 corresponds to land whereas a surface index value of 0 indicates water. Intermediate surface index values are obtained for grid cells containing both land and water (i.e., coastline).

Next, the gridded NIR radiance and surface index data were used to construct a cost function which quantifies the mean radiance over water. The cost function  $C$  to be minimized is

$$C_{m,n} = \sum (1 - S_{i,j})R_{i+m,j+n}$$

where  $m$  and  $n$  are the longitudinal and latitudinal offset indices,  $S_{i,j}$  is the gridded surface index value for longitudinal index  $i$  and latitudinal index  $j$ , and  $R_{i,j}$  is the corresponding gridded 6A radiance value. While the summation is performed over all grid cells (i.e., all  $i$  and  $j$  values) in a given scene, grid cells containing only land do not contribute to  $C$  because of the term  $(1-S)$ . Thus,  $C_{m,n}$  quantifies the mean radiance over water after applying a longitudinal shift of  $m$  grid cells and a latitudinal shift of  $n$  grid cells to the gridded radiances.

The method is illustrated in Fig. 4 below. The top panel shows gridded 6A radiance values (V5) over the eastern Mediterranean Sea and northern Red Sea using all clear-sky observations during 2010. As described in the previous paragraph, the cost function  $C$  was calculated over an array of  $m$ - $n$  indices to determine the latitude/longitude shift which minimizes the mean 6A radiance over water. **For the gridded radiances shown in Fig. 4,  $C$  is minimized for a longitudinal shift of 0.35 degrees ( $m = 7$ ) and a latitudinal shift of 0.0 degrees ( $n = 0$ ). These values are the 'best-fit' values for the MOPITT geolocation bias.** The corrected gridded radiances presented in the bottom panel of Fig. 4 were obtained by shifting the original gridded data by seven grid cells (0.35 degrees) eastward. Similar latitudinal and longitudinal biases, within 0.05 degrees, were derived for other regions (at similar latitudes) and in other years. Based on both the grid resolution and the variability of the results for other years, the uncertainty for the derived latitudinal and longitudinal biases is therefore estimated at 0.05 degrees. No evidence was found that the geolocation biases vary temporally.

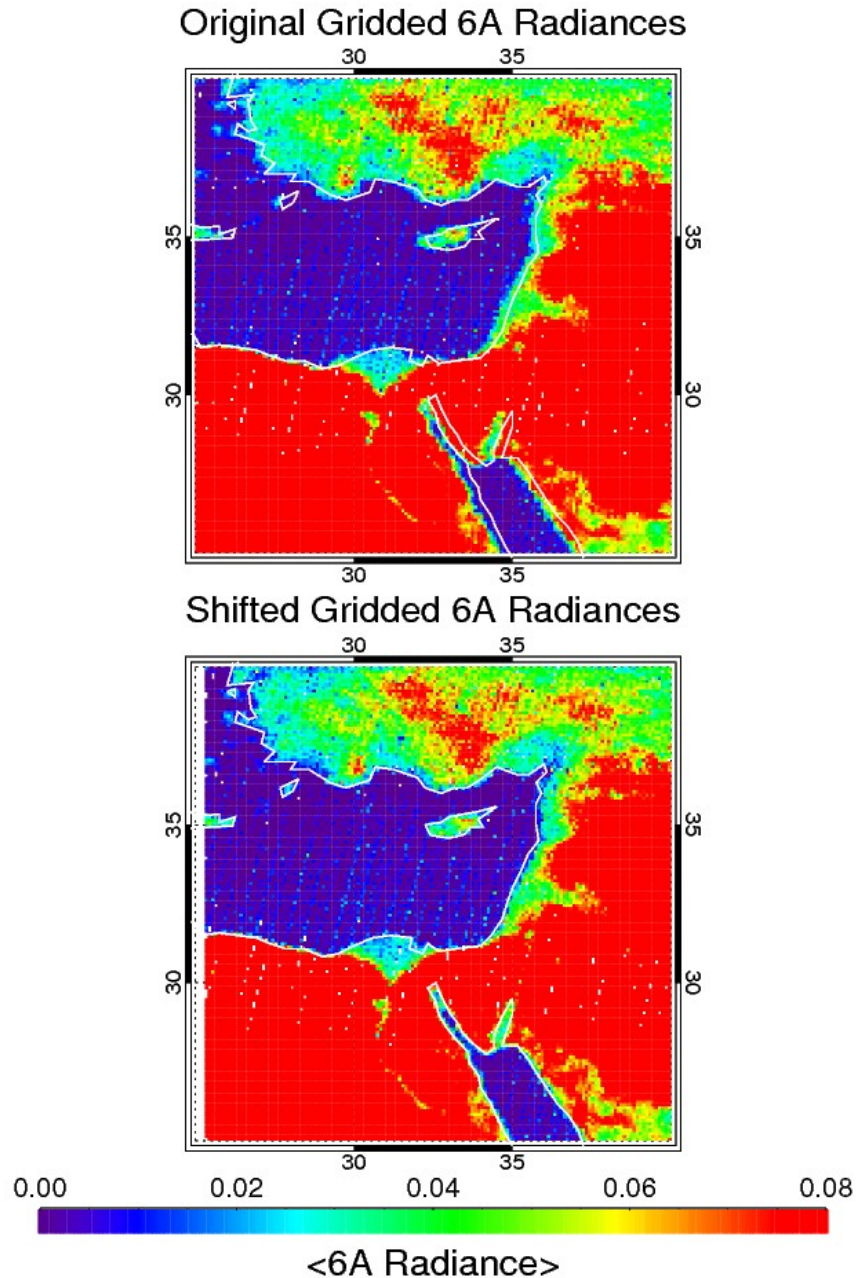


*Figure 4. Gridded 6A clear-sky radiances over the eastern Mediterranean Sea and northern Red Sea for 2010.*

Figures 1 and 2 indicate that geolocation biases for Channels 5 and 6 are quantitatively similar. Maps of single-overpass radiances for Channels 2, 4, 6, and 8 have also been compared for MOPITT observations acquired in the first year of operations. (Channels 2 and 4 were lost as the result of the Side B cooler failure in 2001. Channels 2 and 6 provide NIR measurements of CO, while Channels 4 and 8 provide NIR measurements of methane.) These comparisons indicate quantitatively similar geolocation biases for all the NIR channels. This observation suggests that the MOPITT/Terra

misalignment is not associated with a particular scan mirror, but rather affects the entire instrument.

## 2.2 Method for Quantifying Viewing Angle Bias

Physically, the geolocation bias is most likely the result of a slight misalignment of the MOPITT instrument relative to the Terra platform. Eliminating the bias in future MOPITT products requires that this misalignment be quantified. Thus, the relationship between (1) observed latitudinal and longitudinal biases and (2) viewing-angle biases in both the along-track and cross-track directions must be determined. This relationship is dictated by simple geometrical considerations.

At the center of the region depicted in Fig. 4, for example, a longitudinal bias of 0.35 degrees corresponds to a ground-distance of 32.9 km. When rotated to Terra's coordinate system (which is aligned with the sub-satellite track), this distance can be resolved into an along-track bias of 7.2 km and a cross-track bias of 32.1 km. **Since the Terra platform flies 705 km above the Earth's surface, the estimated along-track angular bias is therefore 0.59 degrees (i.e., 7.2/705 radians) while the estimated cross-track angular bias is 2.61 degrees (32.1/705 radians).** Given that the uncertainties in the latitudinal and longitudinal biases are about 0.05 degrees, the estimated uncertainties in these along-track and cross-track angular biases are both about 0.38 degrees.

## 2.3 Level 1 Processor Revisions

As described in Sec. 1, each MOPITT pixel/stare combination is associated with two offset angles that quantify the along-track and cross-track viewing angles that are unique to that pixel/stare combination. Numerically, these angles are expressed as direction cosines within the 'MOPIP.txt' file. As a key step towards eliminating the effects of the viewing angle biases determined in Sec. 2.2, viewing angles in this file have been revised in an experimental version of the V5 Level 1 Processor. Specifically, for each pixel/stare combination, (1) the direction cosines were converted to actual along-track and cross-track viewing angles, (2) these viewing angles were adjusted to remove the estimated biases (0.59 degrees along-track and 2.61 degrees cross-track) and (3) new direction cosines were calculated and used to replace the original biased values. We then reprocessed one month (June, 2011) of V5 TIR-only product with the revised viewing angles. Comparisons of results with and without the correction are discussed in Sec. 4.

# 3 Additional Effects

As described in this section, the viewing angle bias produces additional secondary effects on MOPITT products beyond simple errors in the latitude and longitude values. Therefore, correcting the bias should improve the quality of MOPITT products in several ways.

## 3.1 Related Geometrical Data

For each MOPITT observation, solar zenith angle and satellite zenith angle values in Level 1 and Level 2 products are determined by calls to the Toolkit, just as latitude and longitude values are. Therefore, the viewing angle bias which produces the geolocation bias should also result in small errors in both the solar zenith and satellite zenith angles. The effects of improved solar and satellite zenith angles on retrieved CO values have not been analyzed.

### **3.2 Cloud Detection**

The cloud detection algorithm for MOPITT retrieval processing employs both (1) MOPITT TIR radiances and (2) the MODIS cloud mask in separate cloud detection tests. The process of matching MOPITT radiances with corresponding MODIS cloud mask data requires accurate geolocation data for both instruments. Thus, if the geolocation data for the MOPITT radiances are biased and the MODIS geolocation values are accurate, cloud detection performance will deteriorate. Specifically, the MODIS component of MOPITT cloud detection will be based on cloud mask values for a region spatially shifted relative to the actual MOPITT observations. An expected result of this effect is that the number of MOPITT retrievals where the MOPITT radiances and MODIS cloud mask both indicate clear-sky should decrease (compared to the ideal case with no geolocation bias). As shown in Section 4, geolocation correction substantially increases the number of retrievals for which MOPITT radiances and the MODIS cloud mask both indicate clear-sky conditions.

Correcting the geolocation data assigned to each Level 1 observation should by itself realign the MOPITT radiances with the MODIS cloud mask and should therefore substantially improve cloud detection performance. On the other hand, the process which subsets the high-resolution MODIS cloud mask to the boundaries of each MOPITT pixel is based on a set of test cases where the geolocation data for both the MOPITT radiances and MODIS cloud mask are assumed to be accurate. The result of this process is a table of relative indices which identify the set of MODIS cloud mask pixels which fall inside the boundaries of a given MOPITT pixel. To fully account for the effects of the geolocation bias on cloud detection, this table has been regenerated with test cases based on corrected geolocation values.

### **3.3 Retrieval Processing**

In addition to the actual radiances, MOPITT retrieval processing depends on several geophysical parameters which vary geographically. The geolocation bias in the Level 1 radiances degrades the process which matches these parameters to Level 1 radiances. Thus, improving the geolocation data for each observation will result in improved CO a priori profiles, a priori surface temperature, surface pressure, and water vapor and temperature profiles. Retrieval quality should benefit from improved geolocation most clearly in locations where these parameters exhibit large horizontal gradients, e.g., over coastlines and mountainous regions.

### **3.4 Level 3 Products**

MOPITT Level 3 Daily and Monthly products are gridded at one-degree resolution (latitude and longitude). Thus, since grid cells are only about three times as large as the geolocation bias, Level 3 products may be significantly affected by the geolocation bias.

## **4 Verification**

While the methodology for quantifying the geolocation bias and corresponding viewing angle bias is based only on daytime NIR radiances over a few regions exhibiting sharp land/ocean contrast, the viewing angle corrections should be equally valid for all geographical regions (i.e., all latitudes) and for both daytime and nighttime overpasses. Below, 6A radiances are compared with and without the geolocation correction in diverse geographical regions. Cloud diagnostics provide additional confirmation of the improvement in geolocation.

#### 4.1 Latitude and Longitude Error Statistics

Latitude and longitude errors were calculated for every retrieval in one full day by subtracting corrected latitude and longitude values from the original biased latitude and longitude values included in the operational V5 product. Figure 5 depicts the latitudinal dependence of these errors. For both latitude and longitude, the figure shows that the errors follow a cyclical pattern corresponding to Terra's polar orbit. The daytime (descending node) and nighttime (ascending node) orbital sections each correspond to one 'lobe' of the closed loops in the two panels. The daytime and nighttime lobes converge near the poles. Thus, for low latitudes, typical daytime latitude errors are near zero whereas typical nighttime latitude errors are about 0.2 degrees. Longitude errors are much larger (in absolute value) than latitude errors, and are slightly larger for daytime overpasses than for nighttime overpasses. These results agree with the conceptual model of the geolocation bias discussed in Sec. 1.3. Latitude and longitude errors also vary slightly with satellite zenith angle; errors tend to increase with increasing satellite zenith angle.

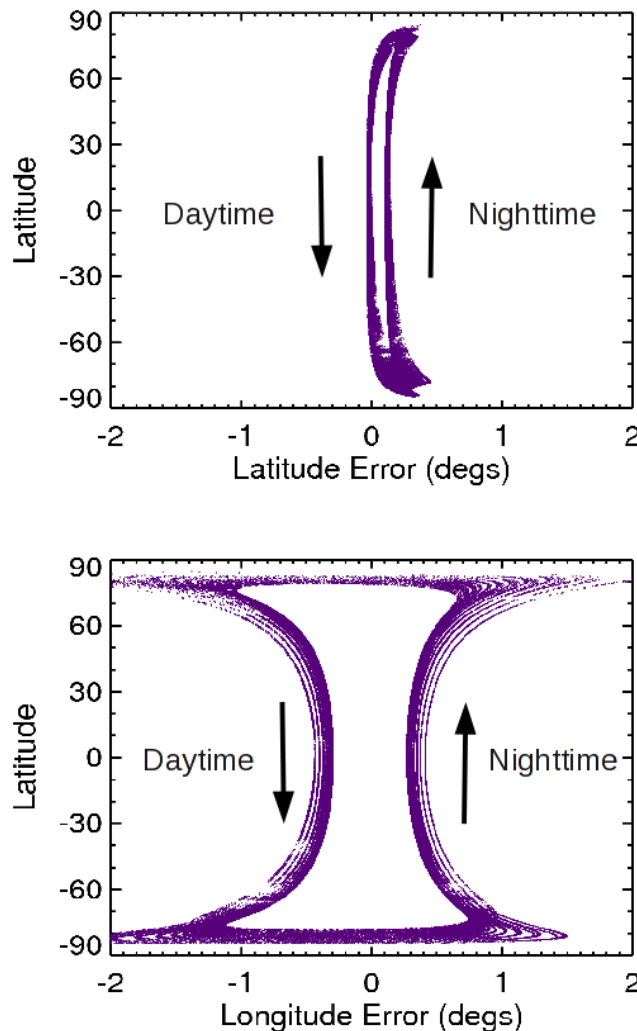


Figure 5. Latitudinal dependence of latitude and longitude geolocation errors calculated for one day.

The errors plotted in Fig. 5 have also been averaged in 10-degree wide latitudinal zones and are listed in Table 1. These mean bias values could be used as the basis of a first-order geolocation correction for current (V4 and V5) operational retrieval products.

Zonal Boundaries		Descending (Daytime)		Ascending (Nighttime)	
Min. Latitude	Max. Latitude	Lat. Error	Lon. Error	Lat. Error	Lon. Error
60N	70N	0.04	-0.74	0.17	0.63
50N	60N	0.13	-0.58	0.14	0.50
40N	50N	-0.01	-0.45	0.13	0.42
30N	40N	-0.01	-0.39	0.12	0.36
20N	30N	-0.02	-0.35	0.12	0.33
10N	20N	-0.02	-0.33	0.12	0.31
Eq.	10N	-0.02	-0.32	0.11	0.31
10S	Eq.	-0.02	-0.32	0.11	0.30
20S	10S	-0.02	-0.34	0.12	0.31
30S	20S	-0.02	-0.36	0.12	0.33
40S	30S	-0.02	-0.39	0.13	0.37
50S	40S	0.00	-0.46	0.13	0.42
60S	50S	0.02	-0.56	0.15	0.49
70S	60S	0.05	-0.82	0.18	0.68

Table 1: Zonal-mean geolocation bias values (in degrees) derived from data plotted in Fig. 5.

## 4.2 Daytime Overpasses

Five daytime scenes representing different geographical regions were selected to verify the improvement in geolocation. Figures A1 to A5 in the Appendix present comparisons of 6A radiances processed with and without the geolocation correction for the following regions: southern Mexico, the Namib desert in southwest Africa, Hudson Bay in northeast Canada, the Cape York Peninsula in northern Australia, and Baja California in northwest Mexico. The top panel in each figure presents the original biased radiances, whereas the bottom panel presents radiances processed with the correction method described in Section 2. In each case, inspection of the corrected radiances along the coastlines indicates that the geolocation correction method greatly reduces the geolocation bias.

## 4.3 Nighttime Overpasses

Geolocation verification is more difficult in nighttime overpasses compared to daytime overpasses because of the lack of solar radiation (which prevents analysis of NIR radiances) and low thermal contrast between ocean and land surfaces at night. On June 29, 2011, however, TIR radiances in nighttime overpasses of Southern Australia and Tasmania exhibit well-defined coastlines separating cold land from warmer ocean. Figure A6 (in the Appendix) compares retrieved surface temperatures before and after applying the geolocation correction for this scene. Again, the geolocation correction

yields radiances in coastal regions which exhibit no obvious geolocation bias.

#### 4.4 Cloud Diagnostics

Another important benefit of geolocation correction is improved cloud detection. The MOPITT cloud detection algorithm involves MOPITT TIR radiances and the MODIS cloud mask. In the current V5 product (and earlier products), the MOPITT TIR radiances exhibit a geolocation bias whereas the geolocation information in the MODIS cloud mask is believed to be accurate. Thus, when determining the cloudiness of a particular MOPITT observation, the MODIS cloud mask data that are exploited are not perfectly registered with the MOPITT observation. This effect should most severely degrade cloud detection in scenes containing broken clouds or cloud edges. In such scenes, the results of cloud tests based on MOPITT's TIR radiances would not be affected while the reliability of the MODIS-based component of cloud detection would decrease.

Table 2 below presents the fractional change in the number of MOPITT retrievals where MOPITT TIR-based cloud detection and the MODIS cloud mask both indicate clear sky (i.e., where the 'Cloud Index' = 2) as the result of the geolocation correction described in Section 2. All observations in June, 2011 were analyzed. Results presented in Table 2 are broken down by day/night and land/ocean. The geolocation correction results in greater consistency between MOPITT and MODIS cloud detection results in all contexts, but particularly over the ocean. The last column in the Table lists the fractional change in the Channel 6A radiance over all daytime/ocean scenes for MOPITT retrievals with a Cloud Index value of 2 (indicating agreement between MOPITT and MODIS). Since the ocean surface is much darker than cloudtops at NIR wavelengths, the 'darkness' of daytime NIR radiances over the ocean provides another quantitative diagnostic for cloud detection performance. For the month of June, 2011, the mean 6A radiance for all daytime/ocean clear-sky observations decreased by 37% as the result of the geolocation correction. Both the increase in MOPITT/MODIS cloud detection agreement and the sharp decrease in NIR radiances in daytime/ocean scenes indicate that the geolocation correction significantly improves cloud detection performance.

*Table 2. Improvements in cloud detection performance for June, 2011 resulting from geolocation correction.*

Fractional Change (in Percent) in MOPITT/MODIS Cloud Detection Agreement				Fractional Change (in Percent) in 6A Radiance
Day/Ocean	Night/Ocean	Day/Land	Night/Land	Day/Ocean
5.9	7.1	2.7	2.0	-37.0

## 5 Summary

Geolocation information in MOPITT products generated since the beginning of the mission until now appear to be biased due to a misalignment between the MOPITT instrument and the Terra platform. A method has been developed to determine the angular misalignment from observations of latitudinal and longitudinal biases in daytime overpasses. The estimated along-track viewing angle bias is 0.59 degrees whereas the estimated cross-track viewing angle bias is 2.61 degrees. The estimated uncertainty in the viewing angle corrections is 0.4 degrees. An experimental Level 1 processor which

explicitly accounts for the viewing angle bias has been developed and used to validate the correction method. Comparisons of MOPITT NIR radiances in various regions before and after the geolocation correction indicate that the method significantly improves the geolocation information. Further evidence of the improved geolocation is provided by analysis of MOPITT cloud diagnostics.

## 6 Appendix

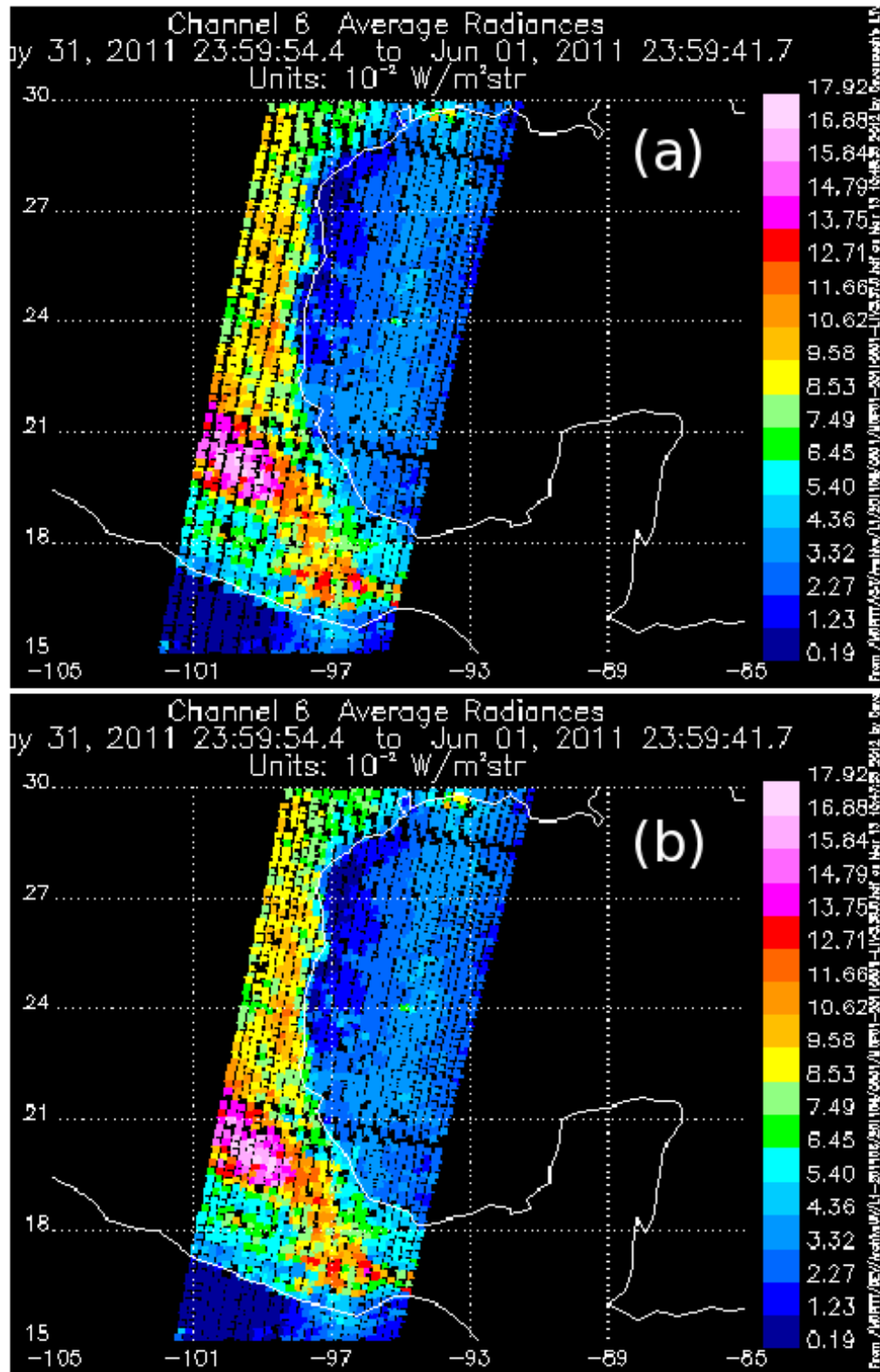


Figure A1. Comparison of 6A radiances before (a) and after (b) geolocation correction for daytime overpass of southern Mexico on June 1, 2011.

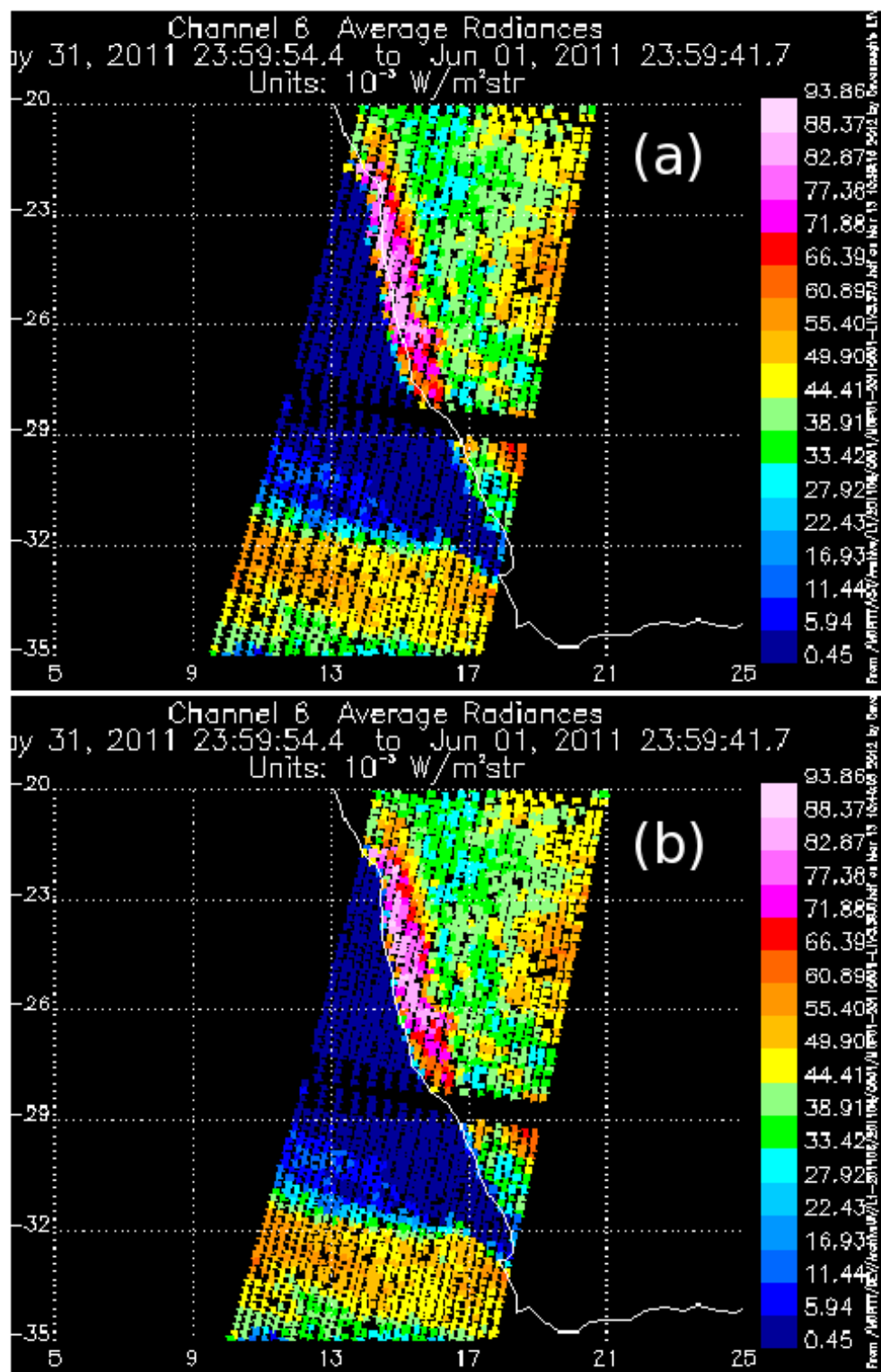


Figure A2. Comparison of 6A radiances before (a) and after (b) geolocation correction for daytime overpass of Namib Desert (Africa) on June 1, 2011.

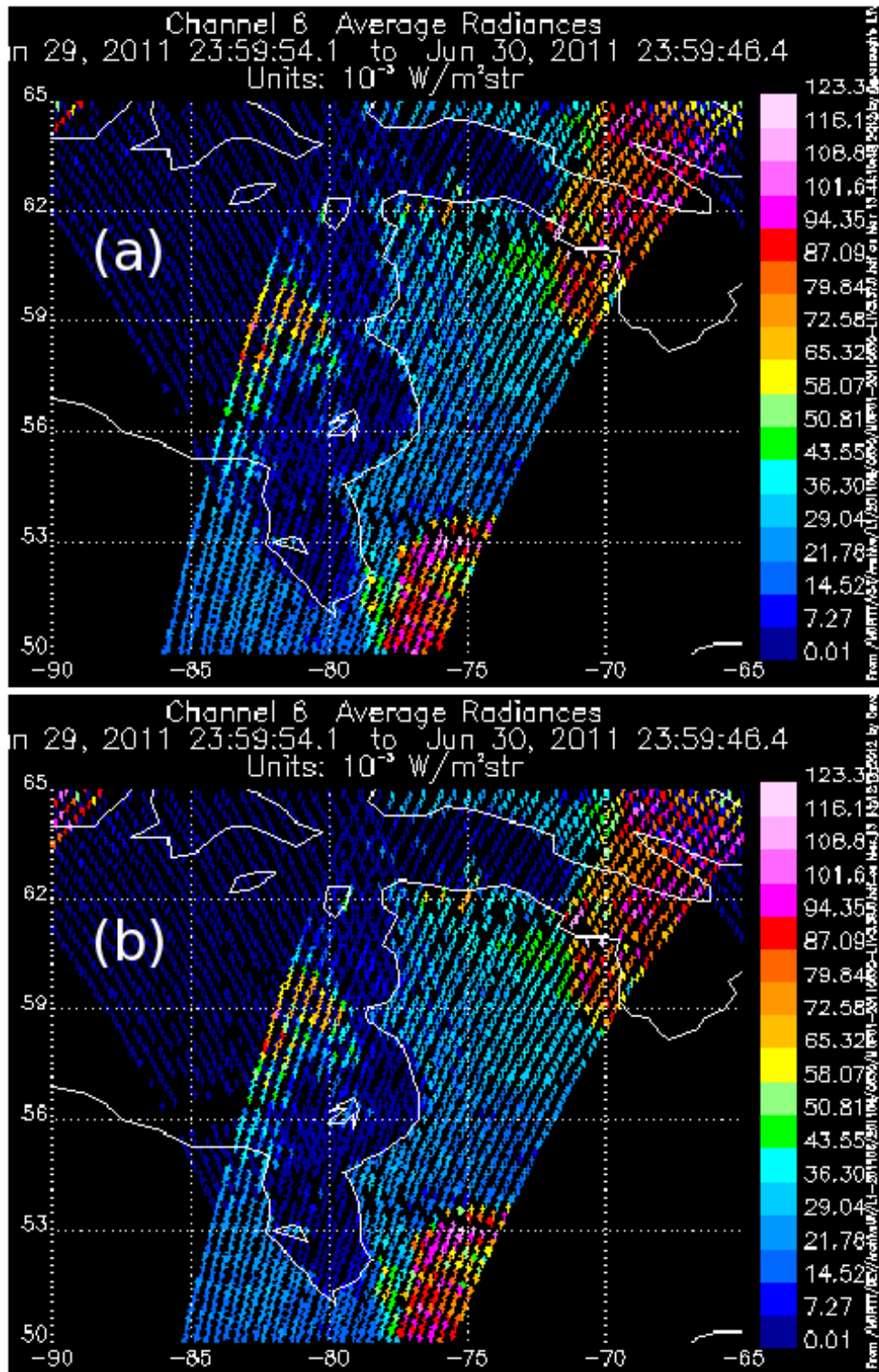


Figure A3. Comparison of 6A radiances before (a) and after (b) geolocation correction for daytime overpass of Hudson Bay (Canada) on June 30, 2011.

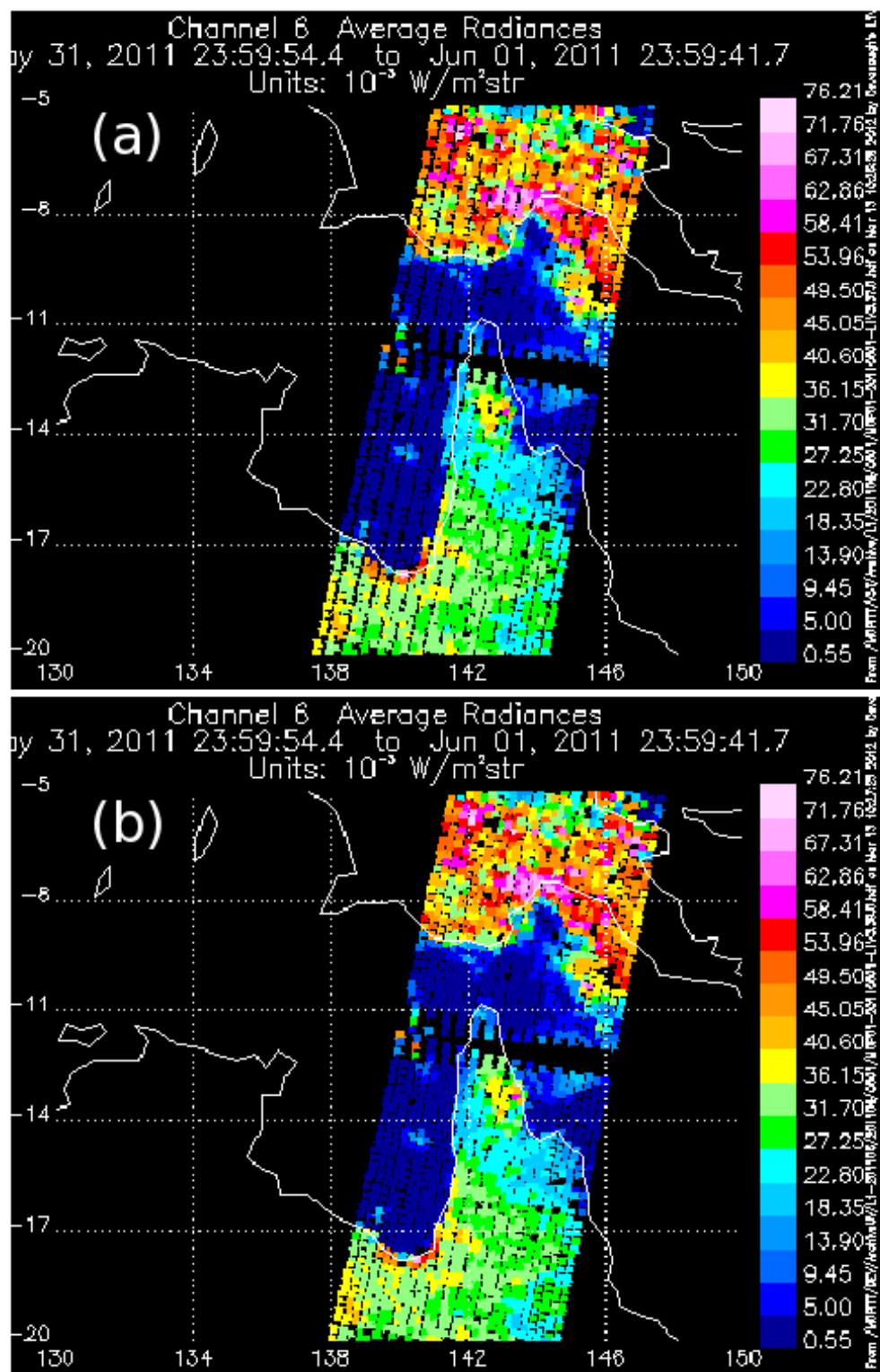


Figure A4. Comparison of 6A radiances before (a) and after (b) geolocation correction for daytime overpass of Cape York Peninsula (Australia) on June 1, 2011.

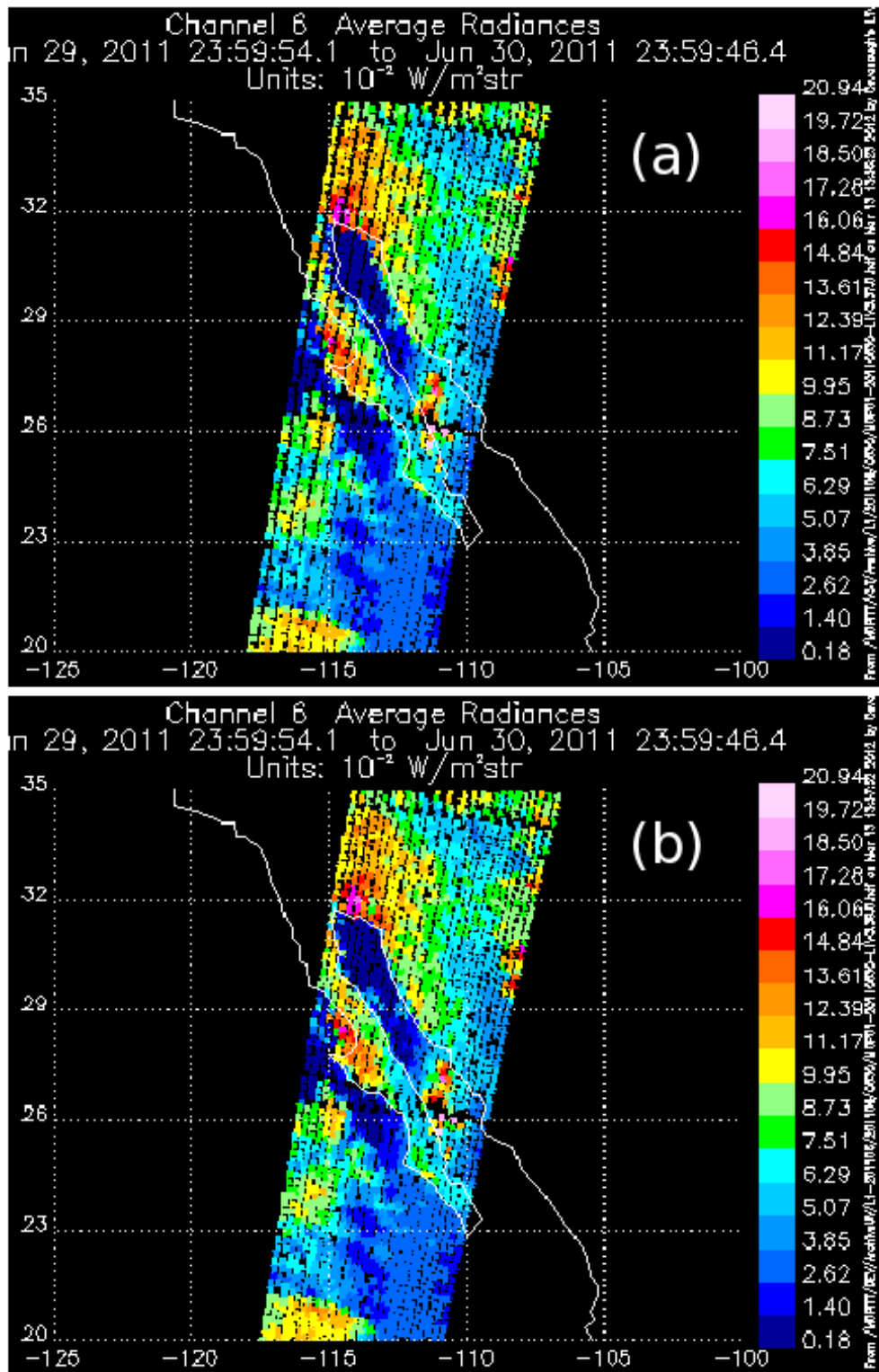


Figure A5. Comparison of 6A radiances before (a) and after (b) geolocation correction for daytime overpass of Gulf of California (Mexico) on June 30, 2011.

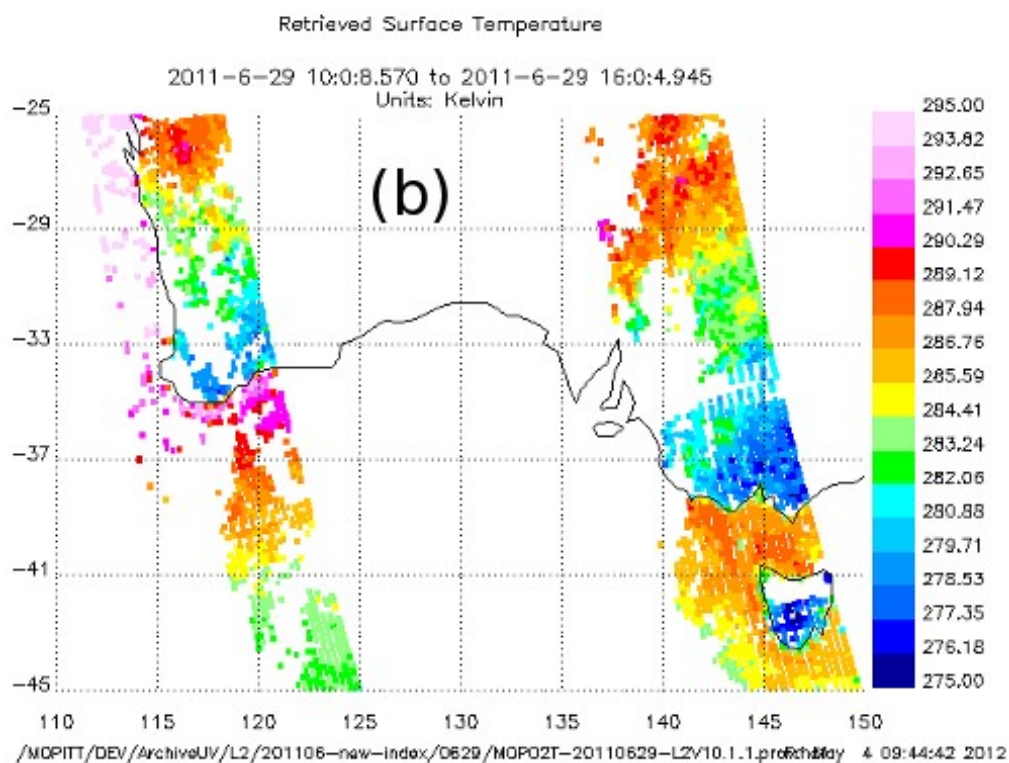
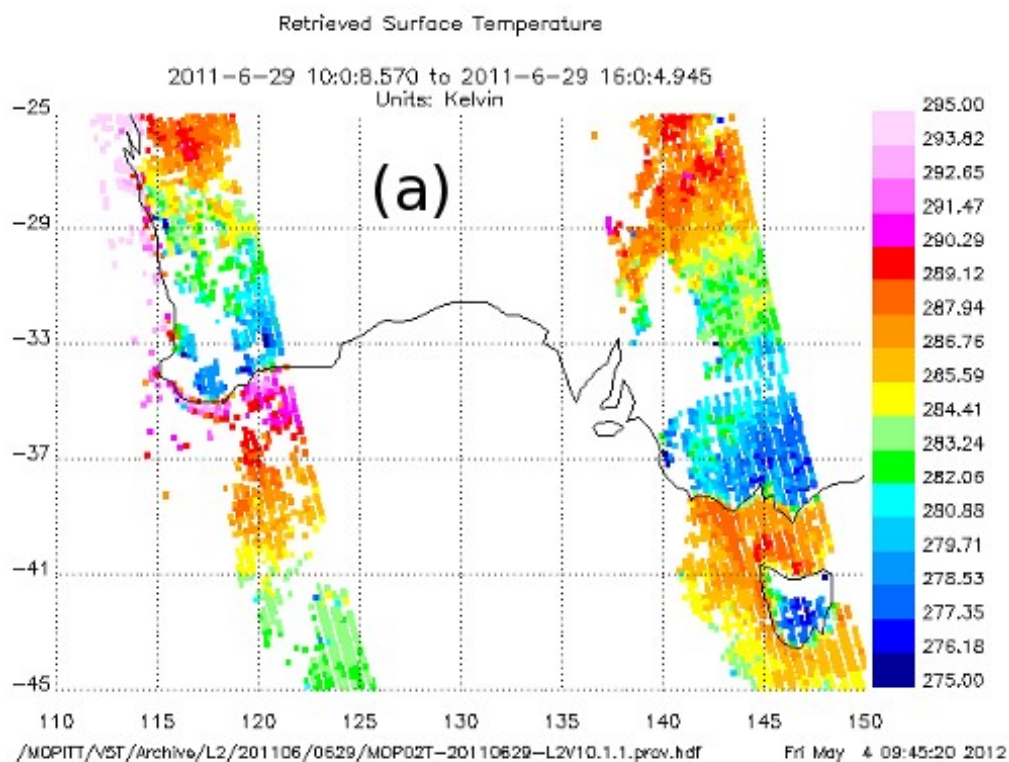


Figure A6. Comparison of retrieved surface temperatures before (a) and after (b) geolocation correction for nighttime overpass of southern Australia and Tasmania on June 29, 2011.